Deep Sequencing in Microdissected Renal Tubules Identifies Nephron Segment–Specific Transcriptomes

Jae Wook Lee, Chung-Lin Chou, and Mark A. Knepper

Epithelial Systems Biology Laboratory, Systems Biology Center, National Heart, Lung and Blood Institute, National Institutes of Health, Bethesda, Maryland

ABSTRACT

The function of each renal tubule segment depends on the genes expressed therein. High-throughput methods used for global profiling of gene expression in unique cell types have shown low sensitivity and high false positivity, thereby limiting the usefulness of these methods in transcriptomic research. However, deep sequencing of RNA species (RNA-seq) achieves highly sensitive and quantitative transcriptomic profiling by sequencing RNAs in a massive, parallel manner. Here, we used RNA-seq coupled with classic renal tubule microdissection to comprehensively profile gene expression in each of 14 renal tubule segments from the proximal tubule through the inner medullary collecting duct of rat kidneys. Polyadenylated mRNAs were captured by oligo-dT primers and processed into adapter–ligated cDNA libraries that were sequenced using an Illumina platform. Transcriptomes were identified to a median depth of 8261 genes in microdissected renal tubule samples (105 replicates in total) and glomeruli (5 replicates). Manual microdissection allowed a high degree of sample purity, which was evidenced by the observed distributions of well established cell–specific markers. The main product of this work is an extensive database of gene expression along the nephron provided as a publicly accessible webpage (https://helixweb.nih.gov/ESBL/Database/NephronRNAseq/index.html). The data also provide genome-wide maps of alternative exon usage and polyadenylation sites in the kidney. We illustrate the use of the data by profiling transcription factor expression along the renal tubule and mapping metabolic pathways.

J Am Soc Nephrol 26: 2669–2677, 2015. doi: 10.1681/ASN.2014111067

The mammalian kidney is made up of thousands of individual nephron units that consist of a glomerulus that generates an ultrafiltrate of blood followed by a long epithelial tubule that modifies the ultrafiltrate by transporting substances into and out of it to form the final urine. The renal tubule is comprised of many segments, each with distinct cell types and functions. Beginning with the work by Burg *et al.*,[1] physiologists have investigated the aggregate function of the kidney by microdissection and study of its component renal tubule segments. Most studies have produced targeted readouts (*e.g.*, transport rates for particular substances, enzyme activities, and content of individual mRNA species). A broader goal, identification of all genes expressed in each cell type, has been pursued with serial analysis of gene expression (SAGE) to identify mRNA transcripts in microdissected tubules.[2,3] This method, however, has limited sensitivity, requiring very large numbers of tubules per sample and limiting the transcriptomic depth (*i.e.*, the number of genes identified per sample). The advent of deep-sequencing (next generation sequencing) technology has provided a quantum leap in sensitivity.[4] This technology, when used for deep sequencing of RNA species (RNA-seq),[5] is sensitive enough to allow large-scale mRNA identification

Received November 4, 2014. Accepted December 17, 2014.

Published online ahead of print. Publication date available at www.jasn.org.

Correspondence: Dr. Mark A. Knepper, National Institutes of Health, Building 10, Room 6N307, 10 Center Drive, MSC-1603, Bethesda, MD 20892-1603. Email: knep@helix.nih.gov

and quantification in a small number of cells.[6,7] In this study, we have used RNA-seq for comprehensive, multireplicate identification of transcriptomes in each of 14 renal tubule segments from rat. These data have been used to create an online resource (https://helixweb.nih.gov/ESBL/Database/NephronRNAseq/index.html). Using this database, we identified unique patterns of distribution of region–specific transcription factors, G protein–coupled receptors, and metabolic enzymes along the renal tubule.

RESULTS

We dissected 14 different renal tubule segments from rat kidneys (Figure 1A). Preliminary RNA-seq runs confirmed successful dissection of specific segments without significant contamination by other cell types (Supplemental Figure 1). However, for a significant number of genes, reads continued beyond the annotated 3′ ends of Ref-seq transcripts (Supplemental Figure 2). To correct these annotations, baseline studies were carried out to map polyadenylation sites in kidney using polyadenylated mRNA sequencing (PA-seq)[8] (Supplemental Datasets 1 and 2).

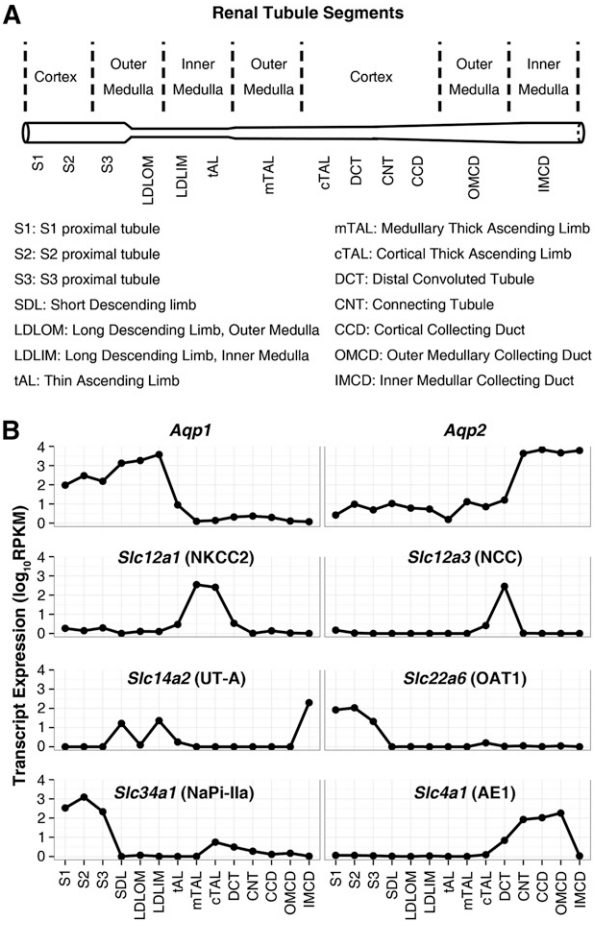

Figure 1. The distribution of RPKM values for several marker genes match prior knowledge, documenting the precision of the technique and the accuracy of segment identification. (A) Nomenclature for renal tubule segments. (B) Median RPKMs for segment-specific markers. *Aqp1*, aquaporin-1; *Aqp2*, aquaporin-2; *Slc4a1* (AE1), anion exchanger 1; *Slc12a1* (NKCC2), bumetanide–sensitive Na^+-K^+-$2Cl^-$ cotransporter; *Slc12a3* (NCC), thiazide–sensitive Na^+-Cl^- cotransporter; *Slc14a2* (UT-A), urea transporter A; *Slc22a6* (OAT1), organic anion transporter 1; *Slc34a1* (NaPi-IIa), sodium-phosphate cotransporter IIa.

We analyzed a total of 105 replicates from 14 renal tubule segments (Supplemental Dataset 1). Gene expression levels of all genes determined by median reads per kilobase of exon model per million mapped reads (RPKM)[9] are provided as a publicly accessible webpage (https://helixweb.nih.gov/ESBL/Database/NephronRNAseq/All_transcripts.html) and spreadsheets (Supplemental Dataset 1). Table 1 summarizes selected characteristics of the data relevant to data quality. The high percentage of mapped reads and the depth of the transcriptomes obtained are consistent with what would be expected for high-quality datasets.[9,10] Reproducibility was documented by hierarchical clustering of all replicates (Figure 2, Supplemental Figure 3). Replicates from the same tubule segment clustered more closely with each other than with those from other segments.

Although not the focus of this study, data from microdissected glomeruli are also provided as a webpage (https://helixweb.nih.gov/ESBL/Database/NephronRNAseq/glomerulus.html) and spreadsheets (Supplemental Dataset 1). Classic glomerular markers, such as nephrin (*Nphs1*) and podocin (*Nphs2*), were found to have high RPKM values in all replicates from glomeruli.

For renal tubule samples, RPKM values ranged over at least four orders of magnitude. For example, in the cortical collecting duct, the water channel aquaporin-2 (*Aqp2*) has a median RPKM of 6776, β-actin (*Actb*) has a median RPKM of 724, and protein kinase A catalytic subunit-β1 (*Prkacb*) has a median RPKM of 11. All of these gene products have important functional roles, despite the wide range of expression levels.

Figure 1B shows median RPKMs of several water and solute transporters plotted as a function of the position along the renal tubule. The distribution of RPKMs of each transcript exactly matched prior knowledge.[11,12] These data provide further documentation for the precision of the technique and the accuracy of segment identification. The renal tubule distributions obtained using RNA-seq showed a high degree of concordance with distributions found using single-tubule RT-PCR for several targets (*viz.*, all three subunits of the epithelial sodium channel [*Scnn1a*, *Scnn1b*, and *Scnn1g*], the basolateral chloride channel ClC-K2 [*Clcnkb*], the urea channel UT-A [*Slc14a2*], and the parathyroid hormone receptor [*Pth1r*]) (Supplemental Material, Supplemental Figure 4).

The single–tubule RNA-seq data provide valuable qualitative information by mapping alternative exon usage for many genes. Figure 3 shows two physiologically important examples. Figure 3A depicts differential use of 5′-end exons between two isoforms of *Fxyd2* that encode the γ-subunit of

Table 1. General characteristics of RNA-seq experiments in microdissected renal tubule segments

Segment	No. of Replicates	Dissected Lengths (mm)	Reads Mapped (%)	Ref-Seq Transcripts with RPKM>0 (without PA-Seq)[a]	Ref-Seq Transcripts with RPKM>0 (with PA-Seq)[a]
G	5	20[b]	89.0–91.8	11,860	12,141
S1	7	0.6–11.8	74.2–93.3	7323	8238
S2	7	2.2–13.0	74.9–90.5	7375	8261
S3	7	1.8–23.6	77.1–91.8	7705	8502
SDL	10	0.8–10.8	77.7–91.2	6305	6995
LDLOM	9	2.6–12.8	75.2–91.7	6125	6933
LDLIM	4	1.4–5.1	83.9–89.1	9005	9649
tAL	7	0.6–8.4	70.0–91.3	8757	9600
mTAL	7	2.6–9.5	83.7–92.5	5895	6659
cTAL	7	1.2–12.2	72.3–92.1	11,146	11,653
DCT	8	2–23[b]	76.9–92.9	9453	10,219
CNT	6	1.2–11.8	70.0–91.1	7573	8409
CCD	11	1.6–12.4	81.5–91.5	8302	9119
OMCD	7	0.8–14.4	82.6–92.3	6880	7601
IMCD	8	0.8–6.7	73.0–92.7	8966	9581

Nomenclature of tubule segments is shown in Figure 1A.
[a]Median numbers.
[b]Number of dissected structures.

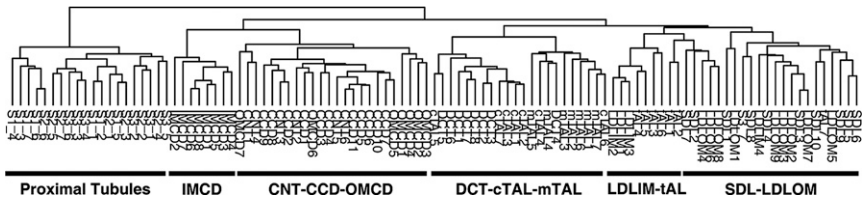

Figure 2. A dendrogram created by hierarchical clustering of 105 replicates of microdissected renal tubule segments demonstrates reproducibility among replicates from the same segment. (Supplemental Figure 3 shows the full heat map representation). Replicates from 14 different renal tubule segments were found to form six distinct clusters according to their anatomic and functional organization. Terminology is the same as in Figure 1A.

the Na^+/K^+-ATPase. The Na^+/K^+-ATPase drives most of the active transepithelial transport across renal tubule segments. The γ-subunit modulates the affinity of the pump for Na^+, K^+, and ATP.[13] The data show that all the segments that display regulated Na^+-Cl^- transport against significant transepithelial gradients (mTAL, cTAL, DCT, CNT, and CCD) use the first alternative initial exon (*Fxyd2b*). In contrast, the segments that do not carry out substantial transepithelial Na^+-Cl^- transport (thin limbs of Henle and IMCD) or carry out unregulated isosmotic Na^+-Cl^- transport (proximal tubule segments) tend to use the second alternative initial exon (*Fxyd2a*). This alternative use of first exons has been suggested to play a role in post-transcriptional regulation of *Fxyd2b* transcripts.[14]

Figure 3B shows two glutaminase (*Gls*) isoforms with alternative carboxyl–terminal amino acid sequences and 3′-untranslated regions. The short isoform predominates in segments downstream from the proximal tubule, but the long isoform is more abundant in proximal tubule. In rats, the 3′-untranslated region of the long isoform contains an AU-rich, pH-responsive element that destabilizes the transcript in the absence of acidosis in some cell types,[15] consistent with the idea that glutaminase enzyme activity is present throughout the renal tubule but regulated only in the proximal tubule.[16]

Table 2 provides a thumbnail view of gene expression along the renal tubule, showing only the transcripts with the highest median RPKM values for each segment in specific gene categories. In addition to water channels and transporters with distributions that are highly consistent with prior knowledge, Table 2 contains a few genes that have no known roles in renal physiology. For example, there are no known roles for the growth hormone–releasing hormone receptor (*Ghrhr*). *Ghrhr* is strongly expressed in the thin descending limb of Henle (SDL and LDLOM). Another example is found among transcripts coding for secreted proteins, namely the abundant expression of defensin-β1 (*Defb1*) in collecting duct segments. Defb1 is an antibacterial protein that is part of the innate immune system.[17]

Cell Type–Specific Transcription Factors

Cell type–specific gene expression depends largely on what combinations of transcription factors are expressed in the cell. For this study, we defined transcription factors as proteins that bind to DNA through a sequence–specific DNA–binding domain and regulate transcription.[18] Of 456 Ref-seq–annotated transcription factors expressed in at least one segment, a subset of highly abundant transcription factors showed distinct patterns of distribution along the renal tubule (Figure 4, Supplemental Figure 5). Several of these showed region-specific expression (Figure 4A), including hepatocyte nuclear factor 4a (*Hnf4a*) in

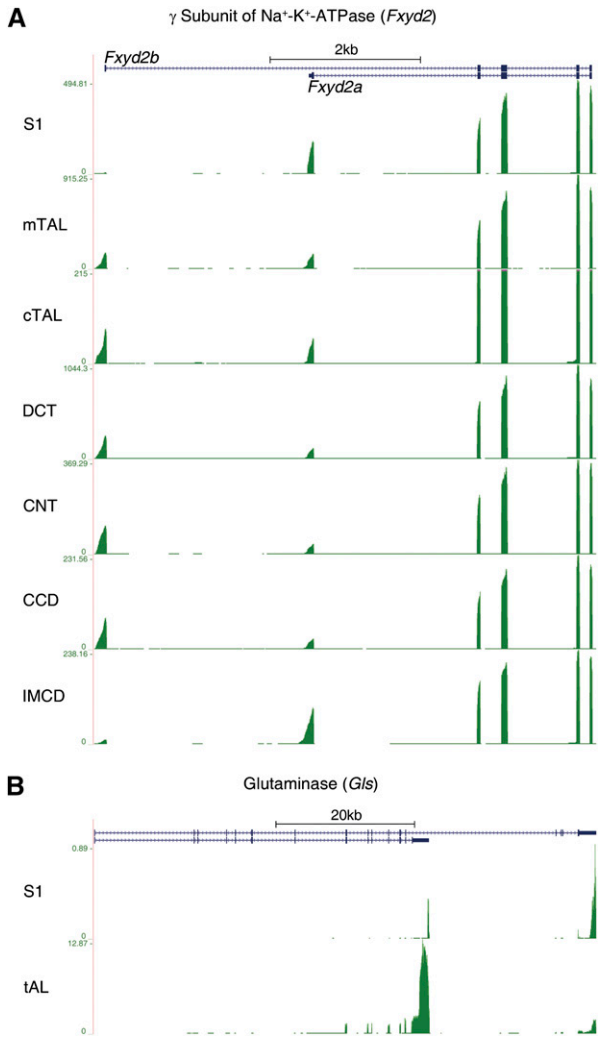

Figure 3. Mapping of deep sequencing reads to gene structure reveals alternative exon usage in different renal tubule segments for some genes. (A) Alternative initial (5′ end) exon usage in the γ-subunit of Na^+-K^+ ATPase (*Fxyd2*). (B) Alternative terminal (3′ end) exon usage in glutaminase (*Gls*).

proximal tubule segments; Iroquois homeobox 5 (*Irx5*) in thin limbs of the loop of Henle; *Irx2* in the thick ascending limbs; and forkhead box i1 (*Foxi1*), H6 homeobox 2 (*Hmx2*), and GATA-binding protein 2 (*Gata2*) in collecting duct segments. Other transcription factors were expressed in two contiguous regions (Figure 4B), including three that had been implicated in cell type–specific gene expression, namely spalt–like transcription factor 1 (*Sall1*), homeobox D10 (*Hoxd10*), and homeobox B7 (*Hoxb7*). The pattern seen for *Hoxb7* is interesting, because this gene is widely considered to be expressed only in the collecting duct system.[19] In fact, the *Hoxb7* promoter is used to target expression to ureteric bud–derived segments in mice. Other transcription factors showed a bimodal pattern, in which there was a skipped region between two regions of high expression (Figure 4, C and D). Most often, these were expressed in thin limbs and collecting ducts. Some of these showed expression in thin limbs and all parts of the collecting duct, including those in the cortical region (Figure 4C). Others showed expression in thin limbs, but collecting duct expression was limited to the inner medullary collecting duct (Figure 4D). This last group has a plausible connection to physiologic factors related to the countercurrent mechanism, namely high osmolality and low oxygen tension.

Critical Enzymes in Metabolic Pathways

Another class of genes for which a deeper analysis of transcript distribution is worthwhile is metabolic enzymes. Although energy metabolism is well understood in proximal tubule segments, few studies have been done in the other renal tubule segments, especially the thin limbs of Henle and the distal convoluted tubule. In a heat map showing the expression of critical enzymes for selected metabolic pathways (Figure 5), the proximal tubule segments stand out as having a unique profile. As is generally accepted, key glycolytic enzymes (hexokinase *Hk1*; phosphofructokinases *Pfkm*, *Pfkl*, and *Pfkp*; and pyruvate kinase *Pkm*) are missing in the proximal tubule, consistent with the view that the proximal tubule does not use glucose

Table 2. Transcripts with the highest expression levels in specific categories

Segment	All Nonhousekeeping Genes[a]	Transporters	G Protein–Coupled Receptors	Protein Kinases	Secreted Proteins
S1	*Gpx3*	*Slc34a1*	*Pth1r*	*Map3k7*	*Sepp1*
S2	*Kap*	*Slc34a1*	*Pth1r*	*Pink1*	*Kap*
S3	*Kap*	*Slc7a13*	*Pth1r*	*Pim3*	*Kap*
SDL	*Spp1*	*Aqp1*	*Ghrhr*	*Tgfbr2*	*Spp1*
LDLOM	*S100a6*	*Aqp1*	*Ghrhr*	*Tgfbr2*	*Spp1*
LDLIM	*Spp1*	*Aqp1*	*Gprc5a*	*Map3k7*	*Spp1*
tAL	*Akr1b1*	*Cldn4*	*Gprc5c*	*Pim3*	*Clu*
mTAL	*Umod*	*Slc12a1*	*Ptger3*	*Map3k7*	*Umod*
cTAL	*Umod*	*Clcnkb*	*Casr*	*Map3k7*	*Umod*
DCT	*Map3k7*	*Slc12a3*	*Ptger3*	*Map3k7*	*Defb1*
CNT	*Aqp2*	*Aqp2*	*Avpr2*	*Map3k7*	*Defb1*
CCD	*Aqp2*	*Aqp2*	*Avpr2*	*Map3k7*	*Defb1*
OMCD	*Aqp2*	*Aqp2*	*Avpr2*	*Sgk1*	*Defb1*
IMCD	*S100a6*	*Aqp2*	*Avpr2*	*Sgk1*	*Guca2a*

Highest RPKM values in each segment. See https://helixweb.nih.gov/ESBL/Database/NephronRNAseq/index.html for a full report of all categories.
[a]Housekeeping genes are those with expression of RPKM>1 in all segments.

for energy metabolism.[20] Also consistent with the generally accepted view, the proximal tubule strongly expresses mRNAs for enzymes that are critical for gluconeogenesis. Glycogen synthase (*Gys1*) was absent, and the enzyme complex that dephosphorylates glucose (*G6pc* and *Slc37a4*) was present, indicating that gluconeogenesis likely results in net glucose production rather than glycogen accumulation. In contrast to the lack of glycolytic enzymes, the key enzymes for fructolysis, namely ketohexokinase (fructokinase *Khk*) and dihydroxyacetone kinase 2 (triokinase *Dak*), are strongly expressed in the proximal tubule. The expression of carnitine palmitoyltransferases was particularly high in the thick ascending limb and distal convoluted tubule, suggesting that fatty acid oxidation may be important in these segments. In addition, argininosuccinate synthase (*Ass1*), necessary for arginine synthesis, was expressed chiefly in the proximal tubule, suggesting that the proximal tubule is responsible for arginine synthesis by the kidney, the major producer of arginine in the body.[21] Little or nothing is known about metabolic processes in thin limb segments. The data suggest that ATP production in the thin limbs, like the more distal segments, is based on glucose metabolism. Hexokinase 1 and phosphofructokinases, critical for glycolysis, are expressed in all segments beyond the proximal tubule. Lactate is also an important substrate in the kidney.[22–24] Isoforms of lactate dehydrogenase showed distinct patterns of expression along the renal tubule (Supplemental Figure 6). The so-called heart isoform, *Ldhb*, that is generally associated with lactate use[25] predominates in the proximal tubule, the thick ascending limb of Henle, and the distal convoluted tubule. The skeletal muscle isoform, *Ldha*, associated with lactate production[25] predominates in all thin limb segments and all collecting duct segments, consistent with the observation that lactate accumulates in the renal medulla.[26] In addition, the

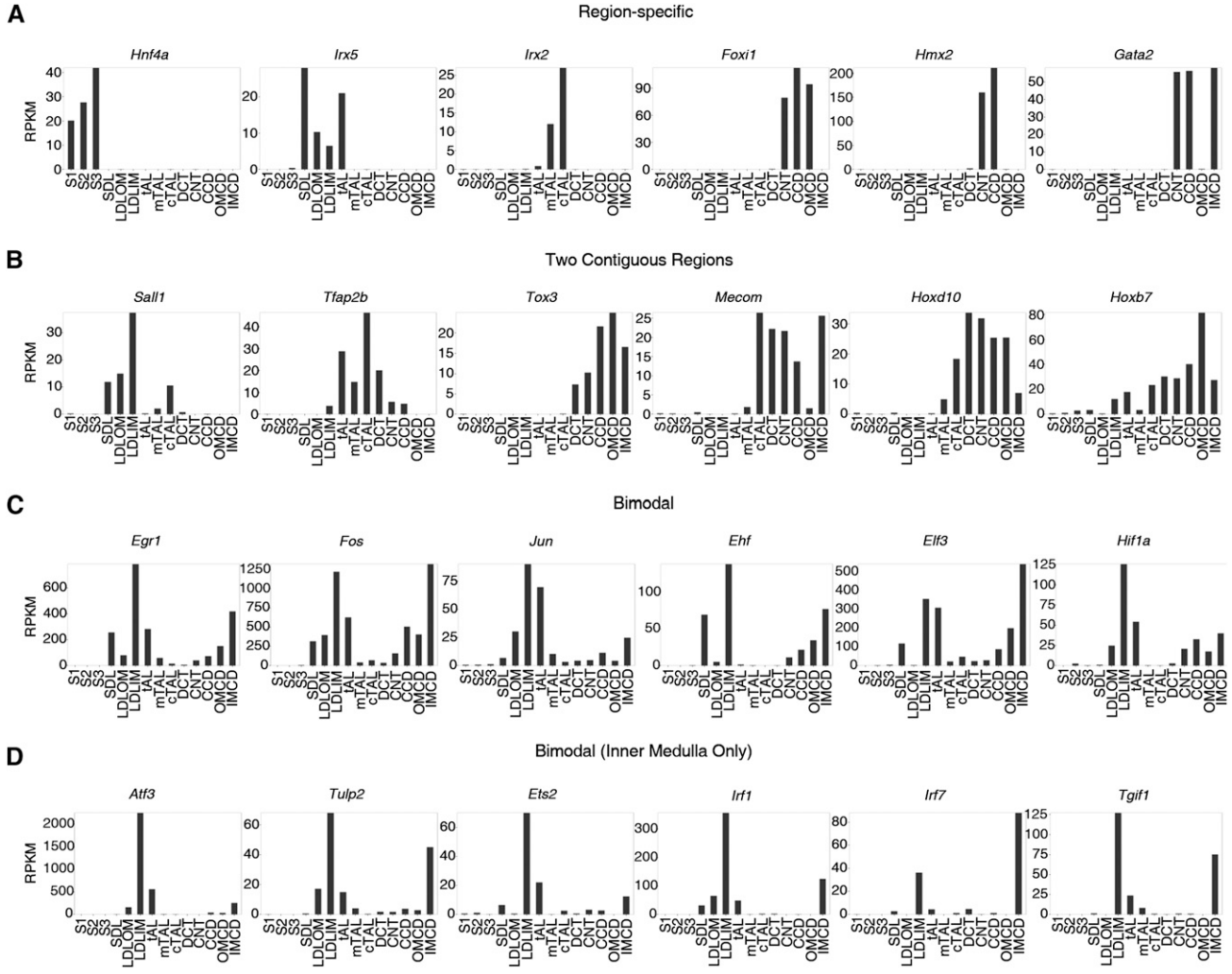

Figure 4. Transcription factors show distinct patterns of expression along the renal tubule. The distributions can be mapped to general regions (proximal region [S1, S2, and S3], thin-limb region, thick-limb/DCT region [mTAL, cTAL, and DCT], and collecting duct region [CNT, CCD, OMCD, and IMCD]). (A) Transcription factors specific to a renal tubule region. (B) Transcription factors expressed in two contiguous regions. (C) Transcription factors with bimodal pattern of expression. (D) Transcription factors with bimodal pattern but expression only in the inner medulla.

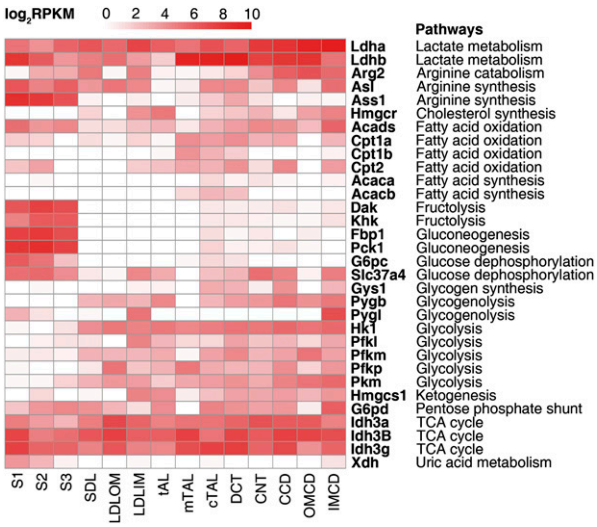

Figure 5. Genes coding for metabolic enzymes are expressed in patterns along the renal tubule that correlate with function. Expression of metabolic enzymes critical for specific metabolic pathways are presented as a heat map showing specific metabolic pathways.

adjacency of the lactate–producing thin descending limbs in the outer medulla to lactate–using medullary thick ascending limbs may be critical to the maintenance of the high rates of active sodium chloride transport in the medullary thick ascending limb needed to drive the countercurrent multiplier mechanism.[27]

Genes Specific to the Nephron and Collecting Duct

The renal tubule is classically divided into two regions on the basis of their developmental origins, namely the nephron (metanephric mesenchyme derived) and the collecting duct (ureteric bud derived). Hierarchical clustering (Concise Methods) identified nephron- or collecting duct–specific transcripts (Figure 6A, Supplemental Dataset 3). One important group of proteins that discriminates between the two regions is secreted proteins. Several secreted proteins seemed to be selectively expressed in the collecting duct segments, namely *Defb1*, glycoprotein hormone-α2 (*Gpha2*), gremlin-1 (BMP antagonist 1 *Grem1*), and guanylate cyclase activator 2a (guanylin *Guca2a*). Each of these has a plausible functional role (Supplemental Dataset 3). Nephron-specific transcripts include a number of abundant secreted proteins, including osteopontin (*Spp1*), kidney androgen–regulated protein (*Kap*), clusterin (*Clu*), activin-binding protein (*Fst*), and trefoil factor 3 (*Tff3*). Interestingly, among nephron-specific transcripts, there were several transcripts for proteins involved in glutathione metabolism and oxidation using molecular oxygen, reflecting known proximal tubule functions (Supplemental Dataset 3).

Genes Enriched in the Medulla

The renal medulla has a parallel structure involving loops of Henle and collecting ducts that is important in the urinary concentrating mechanism. Transcripts enriched in the renal medulla were identified by hierarchical clustering (Figure 6B). In addition to markers of specific cell types (the urea channel *Slc14a2* in thin limbs and IMCD[23] and sodium– and chloride–dependent betaine transporter *Slc6a12* in thin limbs[28]), this heat map shows less well known genes, such as G protein–coupled receptors (*Ghrhr* and *Gprc5a*) and extracellular region–associated proteins (*Fst*, *Ccl7*, and *Cxcl1*). Gene-enrichment analysis (DAVID)[29,30] using 928 genes selectively expressed in the medulla revealed several Gene Ontology (GO) terms (Supplemental Dataset 4), including the extracellular region group. Genes in this group (n=45) included cytokines/chemokines, growth factors, extracellular matrix–associated proteins, proteases, protease inhibitors, ligand antagonists, and hormones (Figure 7). Among these, *Wnt7b* is of particular interest, because it plays a crucial role in the development of the corticomedullary axis and the elongation of the loop of Henle.[31] In our dataset, *Wnt7b* was virtually exclusively expressed in the thin limbs of the loop of Henle and inner medullary collecting ducts.

DISCUSSION

Here, we report the transcriptomic profiling of 14 different renal tubule segments using a combination of classic manual microdissection and RNA-seq. The resulting online database and the data deposited in the Gene Expression Omnibus (GEO) provide useful resources for future studies of renal systems biology, physiology, and development. For example, it can predict labeling patterns for new, previously uncharacterized antibodies, it can provide information about alternative exon usage, it can predict roles for previously unstudied proteins, and it can help us to understand an unexpected phenotype of a transgenic animal. In separate studies, we have reported genome-wide mapping of polyadenylation sites for genes expressed in the kidney, providing reference data for future RNA-seq studies in the kidney.

RNA-seq offers important advantages over other approaches to kidney transcriptomics, such as DNA microarrays using biochemically isolated segments[32,33] or SAGE of microdissected renal tubule segments.[2,3] Compared with biochemical isolation techniques,[34–36] manual dissection virtually eliminates contamination from neighboring segments. RNA-seq does not depend on hybridization and therefore, eliminates false positivity caused by cross-hybridization in microarray studies. Compared with SAGE, RNA-seq offers an approximately two orders of magnitude increase in sensitivity, allowing deep profiling in a few millimeters of microdissected tubules.

This paper provides a limited number of examples of bioinformatic analyses to illustrate some uses of the database. Of particular interest were the profiles of transcription factor expression along the nephron and expression profiles of genes coding for metabolic enzymes. These examples show how transcriptomic profiling along the nephron can fill in the gaps, providing comprehensive information in renal tubules segments that are poorly studied, including the thin limb segments of Henle's loop and the distal convoluted tubule. Also of interest was

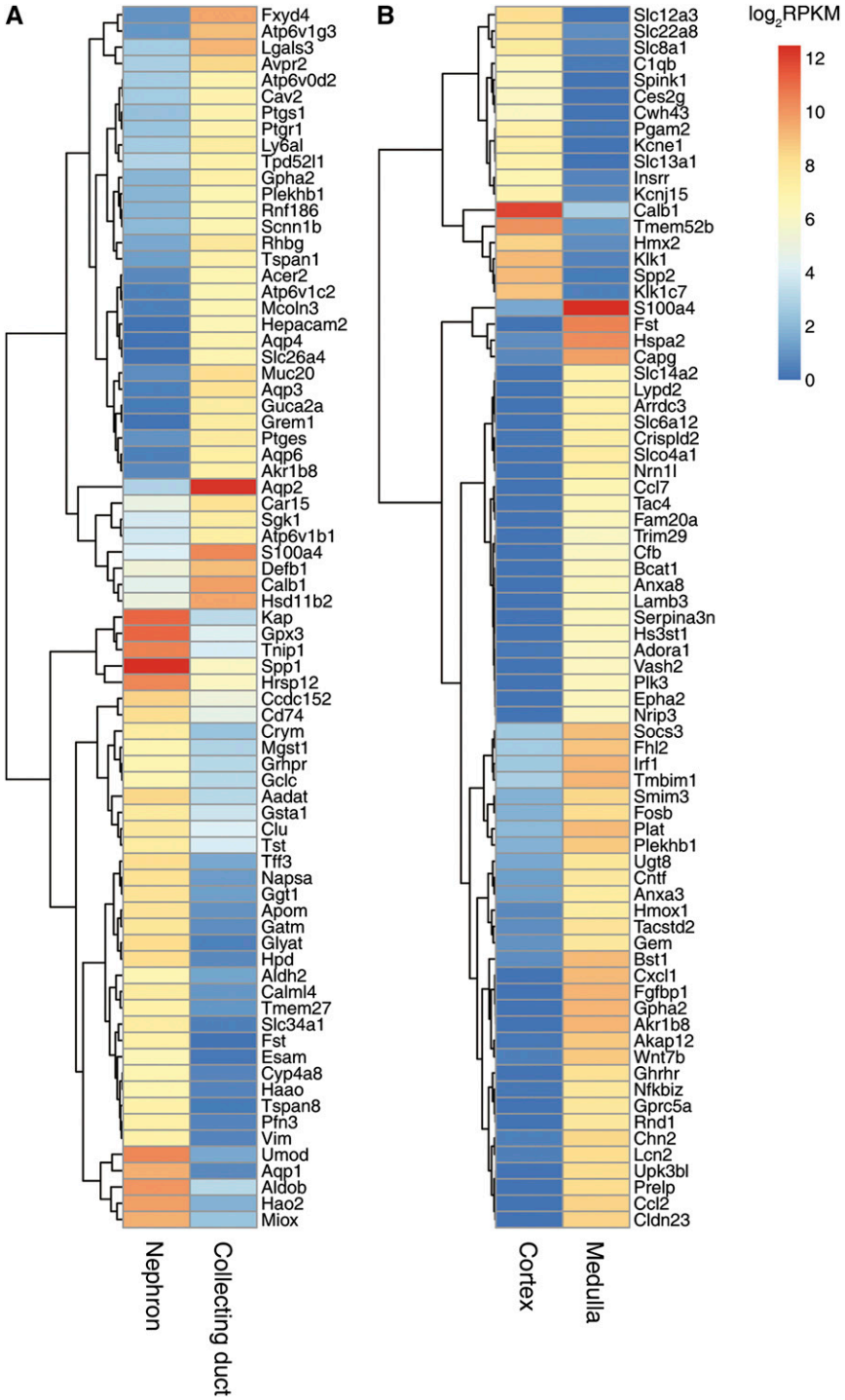

Figure 6. Some transcripts are selectively expressed in developmentally or anatomically defined renal elements. (A) Transcripts selectively expressed in nephron- and collecting duct–derived segments. (B) Transcripts selectively expressed in the cortex and the medulla.

the identification of genes specific to the renal medulla, genes specific to segments derived from the ureteric bud, and genes specific to segments derived from the metanephric mesenchyme. The data can potentially provide useful information for developmental studies, because the adult kidney is the end point of the developmental process.

CONCISE METHODS

Microdissection of Renal Tubule Segments

We followed the standard protocol for microdissection of renal tubule segments from rat kidney.[37] Male Sprague–Dawley rats weighing 200–250 g (Animal Study Protocol No. H-0110R2; approved by the Animal Care and Use Committee, National Heart, Lung, and Blood Institute) were euthanized and processed for microdissection as described in Supplemental Material.

RNA-Seq

Reverse transcription with an oligo-dT primer and cDNA amplification were done following the single–cell RNA-seq protocol.[38] cDNAs were sonicated into approximately 200-bp fragments (Covaris) and made into adapter–ligated cDNA libraries using an Ovation Ultralow Library System (NuGen). cDNAs ranging from 200 to 400 bp were selected on 2% agarose gel and sequenced on a HiSeq2000 platform (Illumina) to generate 50-bp paired-end FASTQ sequences. The raw FASTQ sequences were mapped to the rat reference genome (rn5) using STAR 2.3.0.[39] Only uniquely mapped reads were included in the downstream analysis. RPKMs for Ref-seq transcripts were calculated using the HOMER software.[40] Mapped reads were visualized on the UCSC Genome Browser. RNA-seq library quality was assessed as described by Adiconis *et al.*[41] Basically, RNA-seq library quality in small samples is assessed in terms of the fraction of mapped reads versus total number of reads and the fraction of reads mapped to genomic features (in our case, exons). We used a threshold of 70% of total reads mapped to the reference genome (Supplemental Dataset 1). In this study, 110 of 134 samples met this criterion and are reported in this paper.

PA-Seq

Polyadenylation sites of renal tubule transcripts were identified using a PA-seq protocol reported previously.[8] Ten micrograms DNA–free total RNA prepared from a rat kidney were made into cDNA libraries and sequenced using an Illumina HiSeq2000 platform. RNA-seq reads mapped to the interval between the Ref-seq–annotated 3′ end of the transcript and the tallest PA-seq peak within 5,000 bp downstream from the Ref-seq–annotated 3′ end were included in the calculation of revised RPKM values.

Data Analyses

To identify region–specific gene expression, we calculated the variance of log-transformed RPKMs across the renal tubule segments that

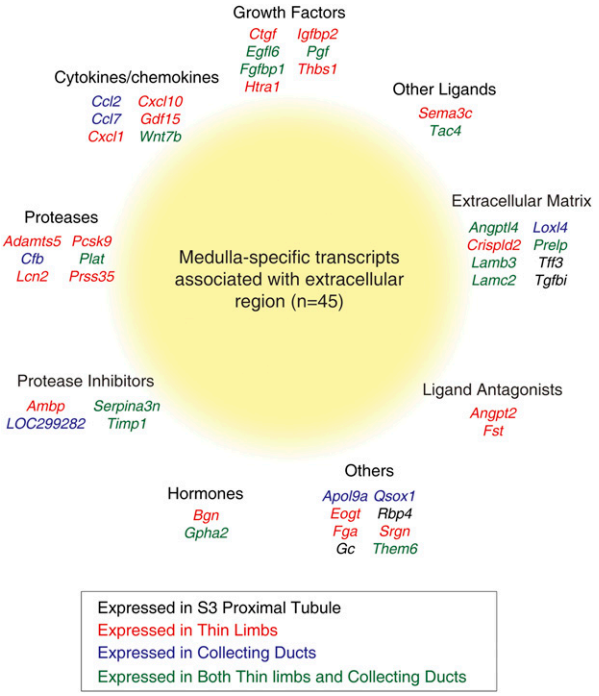

Figure 7. Forty-five medulla-enriched genes are associated with the GO cellular component term 'extracellular region'.

we intended to cluster. Transcripts with the highest variances were selected for hierarchical cluster analysis. Euclidian distances were calculated between $\log_2$-transformed RPKMs, and the complete clustering method was used. For transcription factor analysis, we downloaded a list of rat transcription factors from an online resource (available at http://www.bioguo.org/AnimalTFDB/index.php)[18] and analyzed only Ref-seq–annotated transcription factors (n=456). Graphs and heat maps were drawn using R (http://www.r-project.org) packages ggplot2 and pheatmap. GO term analysis was performed using DAVID.[29] For DAVID analysis of nephron/collecting duct– and cortex/medulla-enriched genes, transcripts at least moderately expressed in either compartment (*i.e.*, mean of RPKMs>10 in either compartment) were used as background (n=3339 for nephron versus collecting duct in Supplemental Dataset 3; n=6943 for cortex versus medulla in Supplemental Dataset 4). In cortex versus medulla, transcripts enriched in GO terms related to the extracellular region (n=91; *e.g.*, 'extracellular region', 'extracellular space', 'extracellular matrix', *etc.*) were further inspected to remove redundant or misannotated transcripts.

Data Availability

The FASTQ sequences and metadata have been deposited in NCBI's GEO (accession no. GSE56743; http://www.ncbi.nlm.nih.gov/geo/query/acc.cgi?acc=GSE56743).

ACKNOWLEDGMENTS

We thank Fahad Saeed for assistance with website construction. Next generation sequencing was done in the National Heart, Lung and Blood Institute (NHLBI) DNA Sequencing and Genomics Core Facility (Jun Zhu, Director).

The work was funded by Division of Intramural Research, NHLBI Projects ZIA-HL001285 and ZIA-HL006129 (to M.A.K.).

Some results were presented at the Annual Meeting of the American Society of Nephrology on October 30–November 4, 2012 (San Diego, CA) and November 5–10, 2013 (Atlanta, GA).

DISCLOSURES

None.

REFERENCES

1. Burg M, Grantham J, Abramow M, Orloff J: Preparation and study of fragments of single rabbit nephrons. *Am J Physiol* 210: 1293–1298, 1966
2. Chabardès-Garonne D, Mejéan A, Aude JC, Cheval L, Di Stefano A, Gaillard MC, Imbert-Teboul M, Wittner M, Balian C, Anthouard V, Robert C, Ségurens B, Wincker P, Weissenbach J, Doucet A, Elalouf JM: A panoramic view of gene expression in the human kidney. *Proc Natl Acad Sci U S A* 100: 13710–13715, 2003
3. Cheval L, Pierrat F, Dossat C, Genete M, Imbert-Teboul M, Duong Van Huyen JP, Poulain J, Wincker P, Weissenbach J, Piquemal D, Doucet A: Atlas of gene expression in the mouse kidney: New features of glomerular parietal cells. *Physiol Genomics* 43: 161–173, 2011
4. Koboldt DC, Steinberg KM, Larson DE, Wilson RK, Mardis ER: The next-generation sequencing revolution and its impact on genomics. *Cell* 155: 27–38, 2013
5. Wang Z, Gerstein M, Snyder M: RNA-Seq: A revolutionary tool for transcriptomics. *Nat Rev Genet* 10: 57–63, 2009
6. Saliba AE, Westermann AJ, Gorski SA, Vogel J: Single-cell RNA-seq: Advances and future challenges. *Nucleic Acids Res* 42: 8845–8860, 2014
7. Tang F, Barbacioru C, Wang Y, Nordman E, Lee C, Xu N, Wang X, Bodeau J, Tuch BB, Siddiqui A, Lao K, Surani MA: mRNA-Seq whole-transcriptome analysis of a single cell. *Nat Methods* 6: 377–382, 2009
8. Ni T, Yang Y, Hafez D, Yang W, Kiesewetter K, Wakabayashi Y, Ohler U, Peng W, Zhu J: Distinct polyadenylation landscapes of diverse human tissues revealed by a modified PA-seq strategy. *BMC Genomics* 14: 615, 2013
9. Mortazavi A, Williams BA, McCue K, Schaeffer L, Wold B: Mapping and quantifying mammalian transcriptomes by RNA-Seq. *Nat Methods* 5: 621–628, 2008
10. Sultan M, Schulz MH, Richard H, Magen A, Klingenhoff A, Scherf M, Seifert M, Borodina T, Soldatov A, Parkhomchuk D, Schmidt D, O'Keeffe S, Haas S, Vingron M, Lehrach H, Yaspo ML: A global view of gene activity and alternative splicing by deep sequencing of the human transcriptome. *Science* 321: 956–960, 2008
11. Agre P, Nielsen S, Knepper MA: Aquaporin water channels in mammalian kidney. In: *The Kidney: Physiology and Pathophysiology*, edited by Seldin DW, Giebisch G, Philadelphia, Lippincott, 2000, pp 363–378
12. Berger UV, Peng J-B, Hediger MA: The membrane transporter families in mammals. In: *The Kidney: Physiology and Pathophysiology*, edited by Seldin DW, Giebisch G, Philadelphia, Lippincott, 2000, pp 107–138
13. Arystarkhova E, Wetzel RK, Asinovski NK, Sweadner KJ: The gamma subunit modulates $Na^{(+)}$ and $K^{(+)}$ affinity of the renal Na,K-ATPase. *J Biol Chem* 274: 33183–33185, 1999
14. Sweadner KJ, Pascoa JL, Salazar CA, Arystarkhova E: Post-transcriptional control of Na,K-ATPase activity and cell growth by a splice variant of FXYD2 protein with modified mRNA. *J Biol Chem* 286: 18290–18300, 2011
15. Ibrahim H, Lee YJ, Curthoys NP: Renal response to metabolic acidosis: Role of mRNA stabilization. *Kidney Int* 73: 11–18, 2008

16. Wright PA, Knepper MA: Phosphate-dependent glutaminase activity in rat renal cortical and medullary tubule segments. *Am J Physiol* 259: F961–F970, 1990
17. Crovella S, Antcheva N, Zelezetsky I, Boniotto M, Pacor S, Verga Falzacappa MV, Tossi A: Primate beta-defensins—structure, function and evolution. *Curr Protein Pept Sci* 6: 7–21, 2005
18. Zhang HM, Chen H, Liu W, Liu H, Gong J, Wang H, Guo AY: AnimalTFDB: A comprehensive animal transcription factor database. *Nucleic Acids Res* 40: D144–D149, 2012
19. Srinivas S, Goldberg MR, Watanabe T, D'Agati V, al-Awqati Q, Costantini F: Expression of green fluorescent protein in the ureteric bud of transgenic mice: A new tool for the analysis of ureteric bud morphogenesis. *Dev Genet* 24: 241–251, 1999
20. Schmid H, Scholz M, Mall A, Schmidt U, Guder WG, Dubach UC: Carbohydrate metabolism in rat kidney: Heterogeneous distribution of glycolytic and gluconeogenic key enzymes. *Curr Probl Clin Biochem* 8: 282–289, 1977
21. Brosnan ME, Brosnan JT: Renal arginine metabolism. *J Nutr* 134[10 Suppl]: 2791S–2795S, 2004
22. Uchida S, Endou H: Substrate specificity to maintain cellular ATP along the mouse nephron. *Am J Physiol* 255: F977–F983, 1988
23. Klein KI, Wang MS, Torikai S, Davidson W, Kurokawa K: Substrate oxidation by defined single nephron segments of rat kidney. *Int J Biochem* 12: 53–54, 1980
24. Nonaka T, Stokes JB: Metabolic support of Na^+ transport by the rabbit CCD: Analysis of the use of equivalent current. *Kidney Int* 45: 743–752, 1994
25. Markert CL: Lactate dehydrogenase. Biochemistry and function of lactate dehydrogenase. *Cell Biochem Funct* 2: 131–134, 1984
26. Scaglione PR, Dell RB, Winters RW: Lactate concentration in the medulla of rat kidney. *Am J Physiol* 209: 1193–1198, 1965
27. Hervy S, Thomas SR: Inner medullary lactate production and urine-concentrating mechanism: A flat medullary model. *Am J Physiol Renal Physiol* 284: F65–F81, 2003
28. Zhou Y, Holmseth S, Hua R, Lehre AC, Olofsson AM, Poblete-Naredo I, Kempson SA, Danbolt NC: The betaine-GABA transporter (BGT1, slc6a12) is predominantly expressed in the liver and at lower levels in the kidneys and at the brain surface. *Am J Physiol Renal Physiol* 302: F316–F328, 2012
29. Huang W, Sherman BT, Lempicki RA: Bioinformatics enrichment tools: Paths toward the comprehensive functional analysis of large gene lists. *Nucleic Acids Res* 37: 1–13, 2009
30. Huang W, Sherman BT, Lempicki RA: Systematic and integrative analysis of large gene lists using DAVID bioinformatics resources. *Nat Protoc* 4: 44–57, 2009
31. Yu J, Carroll TJ, Rajagopal J, Kobayashi A, Ren Q, McMahon AP: A Wnt7b-dependent pathway regulates the orientation of epithelial cell division and establishes the cortico-medullary axis of the mammalian kidney. *Development* 136: 161–171, 2009
32. Yu MJ, Miller RL, Uawithya P, Rinschen MM, Khositseth S, Braucht DW, Chou CL, Pisitkun T, Nelson RD, Knepper MA: Systems-level analysis of cell-specific AQP2 gene expression in renal collecting duct. *Proc Natl Acad Sci U S A* 106: 2441–2446, 2009
33. Uawithya P, Pisitkun T, Ruttenberg BE, Knepper MA: Transcriptional profiling of native inner medullary collecting duct cells from rat kidney. *Physiol Genomics* 32: 229–253, 2008
34. Balaban RS, Soltoff SP, Storey JM, Mandel LJ: Improved renal cortical tubule suspension: Spectrophotometric study of O2 delivery. *Am J Physiol* 238: F50–F59, 1980
35. Chamberlin ME, LeFurgey A, Mandel LJ: Suspension of medullary thick ascending limb tubules from the rabbit kidney. *Am J Physiol* 247: F955–F964, 1984
36. Stokes JB, Grupp C, Kinne RK: Purification of rat papillary collecting duct cells: Functional and metabolic assessment. *Am J Physiol* 253: F251–F262, 1987
37. Wright PA, Burg MB, Knepper MA: Microdissection of kidney tubule segments. *Methods Enzymol* 191: 226–231, 1990
38. Tang F, Barbacioru C, Nordman E, Li B, Xu N, Bashkirov VI, Lao K, Surani MA: RNA-Seq analysis to capture the transcriptome landscape of a single cell. *Nat Protoc* 5: 516–535, 2010
39. Dobin A, Davis CA, Schlesinger F, Drenkow J, Zaleski C, Jha S, Batut P, Chaisson M, Gingeras TR: STAR: Ultrafast universal RNA-seq aligner. *Bioinformatics* 29: 15–21, 2013
40. Heinz S, Benner C, Spann N, Bertolino E, Lin YC, Laslo P, Cheng JX, Murre C, Singh H, Glass CK: Simple combinations of lineage-determining transcription factors prime cis-regulatory elements required for macrophage and B cell identities. *Mol Cell* 38: 576–589, 2010
41. Adiconis X, Borges-Rivera D, Satija R, DeLuca DS, Busby MA, Berlin AM, Sivachenko A, Thompson DA, Wysoker A, Fennell T, Gnirke A, Pochet N, Regev A, Levin JZ: Comparative analysis of RNA sequencing methods for degraded or low-input samples. *Nat Methods* 10: 623–629, 2013

See related editorial, "A Transcriptional Map of the Renal Tubule: Linking Structure to Function," on pages 2603–2605.

This article contains supplemental material online at http://jasn.asnjournals.org/lookup/suppl/doi:10.1681/ASN.2014111067/-/DCSupplemental.

Supplemental Information

RNA-seq in Microdissected Renal Tubules Identifies Nephron Segment-Specific Transcriptomes

Jae Wook Lee[a], Chung-Lin Chou[a], and Mark A. Knepper[a]

[a]Epithelial Systems Biology Laboratory, Systems Biology Center,

National Heart, Lung and Blood Institute, National Institutes of Health, Bethesda, Maryland

Full Methods

Microdissection of Renal Tubule Segments. Male Sprague-Dawley rats weighing 200 - 250 g were euthanized and the left kidney was perfused with bicarbonate-free, ice-cold dissection solution (135 mM NaCl, 1 mM Na_2HPO_4, 1.2 mM Na_2SO_4, 1.2 mM $MgSO_4$, 5 mM KCl, 2 mM $CaCl_2$, 5.5 mM glucose, 5 mM HEPES, pH 7.4) followed by digestion solution containing collagenase B from *Clostridium histolyticum* (Roche Applied Science, 1 mg/mL for cortex and outer medulla, 3 mg/mL for inner medulla) and bovine serum albumin (MP Biomedical, 1 mg/mL for cortex and outer medulla, 3 mg/mL for inner medulla). For outer and inner medulla, hyaluronidase was added (Worthington Biochemical Corporation, 1 mg/mL for cortex and outer medulla, 3 mg/mL for inner medulla). The left kidney was removed and small chunks of the tissue were incubated in the same digestion solution at 37°C for 25 minutes (cortex), 50 minutes (outer medulla), or 90 minutes (inner medulla). Tubule microdissection was carried out using a Wild M8 dissection stereomicroscope (Wild Heerbrugg) that transmitted light from below a specially designed microdissection table. This technique allows each renal tubule segment to be discriminated based on its appearance and topology.[1] Nomenclature for individual segments is given in Supplemental Figure 1A. For the proximal tubule segments, S1 was identified as the proximal tubule directly attached to the glomerulus, S2 was the straight part in the medullary ray, and S3 was the proximal tubule in the outer medulla. The short descending thin limb (SDL) and long descending thin limb of the outer medulla (LDLOM) were identified by their direct attachment to the S3 segment, and distinguished from each other based on their diameters and surface appearance. The long descending thin limb of the inner medulla (LDLIM) and the thin

ascending limb (tAL) were dissected from the inner medulla. The thin ascending limb was identified by its attachment to the medullary thick ascending limb. The medullary thick ascending limbs (mTALs) were dissected from the inner stripe of the outer medulla. The cortical thick ascending limbs (cTALs) were dissected from the medullary rays of the cortex. The distal convoluted tubule (DCT) was defined as a V-shaped or convoluted segment beyond the macula densa. The DCT was typically uniform in appearance for about 1 mm and underwent a gradual transition to the connecting tubule. We took only the uniform portion of the DCT. The transition region, sometimes referred to as DCT2, was discarded. The connecting tubule was identified by its cobblestone appearance and branching structure. The cortical collecting duct (CCD) was dissected from the medullary rays of the cortex. The outer medullary collecting duct (OMCD) was dissected chiefly from the inner stripe of the outer medulla. The inner medullary collecting duct (IMCD) was dissected from the middle portion of the inner medulla. Typically, several dissected tubules were pooled for one sample, yielding 4 - 5 mm of total tubule length. This would correspond to 1,000 - 2,000 cells per sample.

Construction of cDNA libraries for RNA-seq. Dissected tubule segments were transferred using long pipette tips, washed in 1× phosphate-buffered saline (PBS) under a second dissection microscope (Wild M8 stereomicroscope, Wild Heersbrugg), and transferred to a 0.5-mL PCR tube (Sorenson Bioscience) in ~2 μL of PBS. Based on prior experience, this wash step was crucial for elimination of contaminating cells. Reverse transcription with an oligo-dT primer and cDNA amplification were done following the single-cell RNA-seq protocol.[2] For this protocol, reverse transcription requires oligo-dT primers rather than random hexamers since there is no mRNA

extraction step. For cell lysis, 20 μL of cell lysis buffer as prepared according to (ref. 2) was added to the collected tubule segments. The tube was then centrifuged for 30 s at 7,500 g at 4 °C, incubated at 70 °C for 90 s to release mRNA, and then centrifuged again for 30 s at 7,500 g at 4 °C. To start first-strand synthesis, we added 0.55 μL of cell lysate and 0.45 μL of reverse transcriptase mix [SuperScript III reverse transcriptase (13.2 U/μL, Invitrogen); RNase inhibitor (0.4 U/μL, Ambion); and T4 gene 32 protein (0.07 U/μL, Roche Applied Science)] to 4 μL of the cell lysis buffer. After first-strand synthesis, free primers were removed using exonuclease I (0.5 U/μL, New England Biolabs), poly(A)' tails were added to the 5'-ends of the DNA-RNA hybrid using dATP (3 mM, Invitrogen) and terminal transferase (0.75 U/μL, Invitrogen), and RNA template was removed using RNase H (0.1 U/ μL, Invitrogen). Second-strand synthesis was carried out using a pair of universal primers (1μM UP1, 5'-ATATGGATCCGGCGCGCCGTCGACTTTTTTTTTTTTTTTTTTTTTTT-3'; 1 μM UP2, 5'-ATATCTCGAGGGCGCGCCGGATCCTTTTTTTTTTTTTTTTTTTTTTT-3', Eurofins Genomics), dNTPs (0.25 mM each) and ExTaq HS DNA polymerase (0.05 U/μL, Clontech). The first-round PCR amplification (20 cycles) was performed using the same primers and DNA polymerase. For the second-round PCR (9 cycles), the primers were switched to 5'-NH_2-modified primers with the same nucleotide sequences as above to minimize the amount of the primers in the final RNA-seq libraries. Specifications of thermal cycles used in the above procedures are provided in [2]. After reverse transcription and amplification, cDNAs ranging from 100 to 3000 bp in length were selected on 2% agarose E-gels (Life Technologies) and extracted using Zymo Gel DNA Recovery kit (Zymo Research). Concentrations of cDNAs were measured using a Qubit

fluorometer (Life Technologies). Three hundred nanograms of cDNAs were sheared to generate ~200 bp fragments using a Covaris S2 sonication system (Covaris) according to the manufacturer's protocol. Sheared cDNAs were made into adapter-ligated cDNA libraries using an Ovation Ultralow library system (NuGen) and a Mondrian SP+ microfluidic sample preparation system (NuGen) following manufacturer's protocols. cDNAs ranging from 200 to 400 bp were selected on 2% agarose E-gel and recovered using Zymo Gel DNA Recovery kit. Paired-end sequencing was carried out on a HiSeq2000 platform (Illumina) to generate 50-bp FASTQ sequences.

Mapping to the rat reference genome. The raw FASTQ sequence files were inspected and nucleotides with sequencing quality score less than 30 (phred33) were trimmed using Trimmomatic 0.3.2[3], available at http://www.usadellab.org/cms/?page=trimmomatic. FASTQ sequences that passed this test were mapped to the rat reference genome (rn5) using Spliced Transcripts Alignment to a Reference (STAR) version 2.3.0.[4] A genomic index for rat was built from FASTA sequences of rat chromosomes (including 'random' assemblies) downloaded from the UCSC table browser website, and the FASTQ sequences were mapped to the rat reference genome using the following command: STAR --genomeDir <*genomedirectory*> --readFilesIn <*file1.fastq*> <*file2.fastq*> --runThreadN 8 --outFilterMismatchNmax 3 --genomeLoad LoadAndKeep --outSAMstrandField intronMotif --alignIntronMax 10000 --alignMatesGapMax 10000 --outFilterIntronMotifs RemoveNoncanonicalUnannotated. RNA-seq samples with <70% of mappability (i.e. fraction of reads mapped to the reference genome) were discarded. Only uniquely mapped reads were included in the downstream analysis. The numbers of mapped

reads and RPKMs for RefSeq transcripts were calculated using the HOMER software package.[5] To revise gene expression for a RefSeq transcript, RNA-seq reads in the interval between the RefSeq-annotated 3'-end and the PA-seq peak were included in calculating RPKMs. Mapped reads were converted to bedgraph format and visualized on the UCSC Genome Browser.

Polyadenylated mRNA-seq (PA-seq). To identify polyadenylation sites of renal tubule transcripts, we used a PA-seq protocol developed by the DNA Sequencing and Computational Biology Core of the National Heart, Lung, and Blood Institute [6]. This protocol captures nucleotide sequences at polyadenylation sites and sequences them in a strand-specific, paired-end manner. Ten micrograms of DNA-free total RNA prepared from a rat kidney using RNEasy Mini kit (QIAGEN) were made into a strand-specific cDNA library. This PA-seq library was sequenced using the Illumina HiSeq2000 platform and processed as described in [6] to call polyadenylation peaks. To revise the RPKM value for an underannotated RefSeq transcript, we included RNA-seq reads that mapped to the interval between the RefSeq-annotated 3'-end of the transcript and the tallest PA-seq peak within 5,000 bp downstream from the RefSeq-annotated 3'-end.

Supplemental Discussion

Comparison of Results from Single-Tubule RNA-seq with RT-PCR Results for Specific Gene Targets

To provide further evidence that the single-tubule RNA-seq method gives reliable expression profiles along the renal tubule, we compare RNA-seq data with RT-PCR results from microdissected segments in what follows.

Epithelial Sodium Channel (ENaC) Subunits. The epithelial sodium channel is a heterotrimer made of three subunits: α, β, and γ (official gene symbols: *Scnn1a, Scnn1b* and *Scnn1g,* respectively). Within the kidney, it is generally accepted that the epithelial sodium channel has its major functional role in the principal cells of the collecting duct and connecting tubule where it mediates aldosterone dependent regulation of sodium ion reabsorption. Our RNA-seq analysis shows that all three ENaC subunits are expressed in the CNT, CCD, and OMCD, consistent with the generally held view (Supplemental Figure 4A). In addition, the expression of αENaC extends upward along the renal tubule to the DCT, cTAL and mTAL. Beyond this, there is expression of the beta subunit in the DCT and cTAL. Thus, according to the RNA-seq analysis, the only subunit that is uniquely expressed in principal cell-containing segments is the γ subunit. This pattern agrees with a prior study [7] that used single-tubule RT-PCR to localize ENaC subunit expression (Supplemental Figure S6A). Although not all segments were studied and a different animal species was used, the general pattern was seen to be the same as for our RNA-seq results in rats. Specifically, (a) significant levels of α-ENaC

mRNA are detectable upstream from the collecting duct, viz. in mTAL, cTAL, and DCT, and (b) γ-ENaC mRNA had the most restricted distribution with consistently detectable levels only in the CNT, CCD, and OMCD. Another study used in situ RT-PCR hybridization to localize mRNA for α subunit. This study also showed expression of the α subunit of ENaC in the mTAL and DCT in addition to CNT and collecting duct segments [8]. In conclusion, there appeared to be general agreement between RNA-seq results and RT-PCR results with regard to distribution of ENaC subunits along the renal tubule.

Basolateral Chloride Channel ClC-K2. ClC-K2 (gene symbol: *Clcnkb*) is a chloride channel expressed in the basolateral plasma membrane in distal nephron segments and in collecting ducts. It is believed to constitute the major pathway for basolateral chloride exit in transepithelial Na-Cl reabsorption in distal nephron and collecting duct. There was a very high degree of concordance between our RNA-seq data and the RT-PCR result [9] (Supplemental Figure S6B).

Urea Channels UT-A1, UT-A2 and UT-A3. Urea channel proteins play important roles in the urinary concentrating mechanism. All three urea channel mRNAs (UT-A1, UT-A2 and UT-A3) are coded by the *Slc14a2* gene, differing on the basis of differential promoter utilization and differential splicing. The distribution of RPKM values mapped to *Slc14a2* is shown in Supplemental Figure S6C. Mapping of RNA-seq data does not readily discriminate between UTA1 and UT-A2 because they have a common 3'-end. Previous RT-PCR studies in microdissected renal tubule segments found UT-A1 mRNA in the IMCD and UT-A2 mRNA in the SDL and LDLIM but did not identify transcripts in LDLOM, exactly matching the distribution shown in Supplemental Figure 1B [10] (The RT-

PCR study did not attempt to identify UT-A3 transcripts). Thus, there was a high degree of concordance between RNA-seq data and RT-PCR data for *Slc14a2* transcripts.

Parathyroid Hormone Receptor (*Pth1r*). The parathyroid hormone receptor is a G protein-coupled receptor that mediates effects of parathyroid hormone on transport processes in the kidney. Supplemental Figure S6D shows the distribution of *Pth1r* mRNA along the renal tubule based on RNA-seq experiments report in the present paper (left) and the distribution obtained by semiquantitative RT-PCR in microdissected segments from rats based on multiple replicates (right, [11]). There appears to be a high degree of concordance between the expression patterns obtained with the two methods.

References

1. Wright PA, Burg MB, Knepper MA: Microdissection of kidney tubule segments. *Methods Enzymol* 191**:** 226-231, 1990.

2. Tang F, Barbacioru C, Nordman E, Li B, Xu N, Bashkirov VI, Lao K, Surani MA: RNA-Seq analysis to capture the transcriptome landscape of a single cell. *Nat Protoc* 5**:** 516-535, 2010.

3. Bolger AM, Lohse M, Usadel B: Trimmomatic: A flexible trimmer for Illumina Sequence Data. *Bioinformatics*, 2014.

4. Dobin A, Davis CA, Schlesinger F, Drenkow J, Zaleski C, Jha S, Batut P, Chaisson M, Gingeras TR: STAR: ultrafast universal RNA-seq aligner. *Bioinformatics* 29**:** 15-21, 2013.

5. Heinz S, Benner C, Spann N, Bertolino E, Lin YC, Laslo P, Cheng JX, Murre C, Singh H, Glass CK: Simple combinations of lineage-determining transcription factors prime cis-regulatory elements required for macrophage and B cell identities. *Mol Cell* 38**:** 576-589, 2010.

6. Ni T, Yang Y, Hafez D, Yang W, Kiesewetter K, Wakabayashi Y, Ohler U, Peng W, Zhu J: Distinct polyadenylation landscapes of diverse human tissues revealed by a modified PA-seq strategy. *BMC Genomics* 14**:** 615, 2013.

7. Velazquez H, Silva T, Andujar E, Desir GV, Ellison DH, Greger R: The distal convoluted tubule of rabbit kidney does not express a functional sodium channel. *Am J Physiol Renal Physiol* 280**:** F530-539, 2001.

8. Ciampolillo F, McCoy DE, Green RB, Karlson KH, Dagenais A, Molday RS, Stanton BA: Cell-specific expression of amiloride-sensitive, Na(+)-conducting ion channels in the kidney. *Am J Physiol* 271**:** C1303-1315, 1996.

9. Vitzthum H, Castrop H, Meier-Meitinger M, Riegger GA, Kurtz A, Kramer BK, Wolf K: Nephron specific regulation of chloride channel CLC-K2 mRNA in the rat. *Kidney Int* 61**:** 547-554, 2002.

10. Shayakul C, Knepper MA, Smith CP, DiGiovanni SR, Hediger MA: Segmental localization of urea transporter mRNAs in rat kidney. *Am J Physiol* 272**:** F654-660, 1997.

11. Yang T, Hassan S, Huang YG, Smart AM, Briggs JP, Schnermann JB: Expression of PTHrP, PTH/PTHrP receptor, and Ca(2+)-sensing receptor mRNAs along the rat nephron. *Am J Physiol* 272**:** F751-758, 1997.

Supplemental Figures.

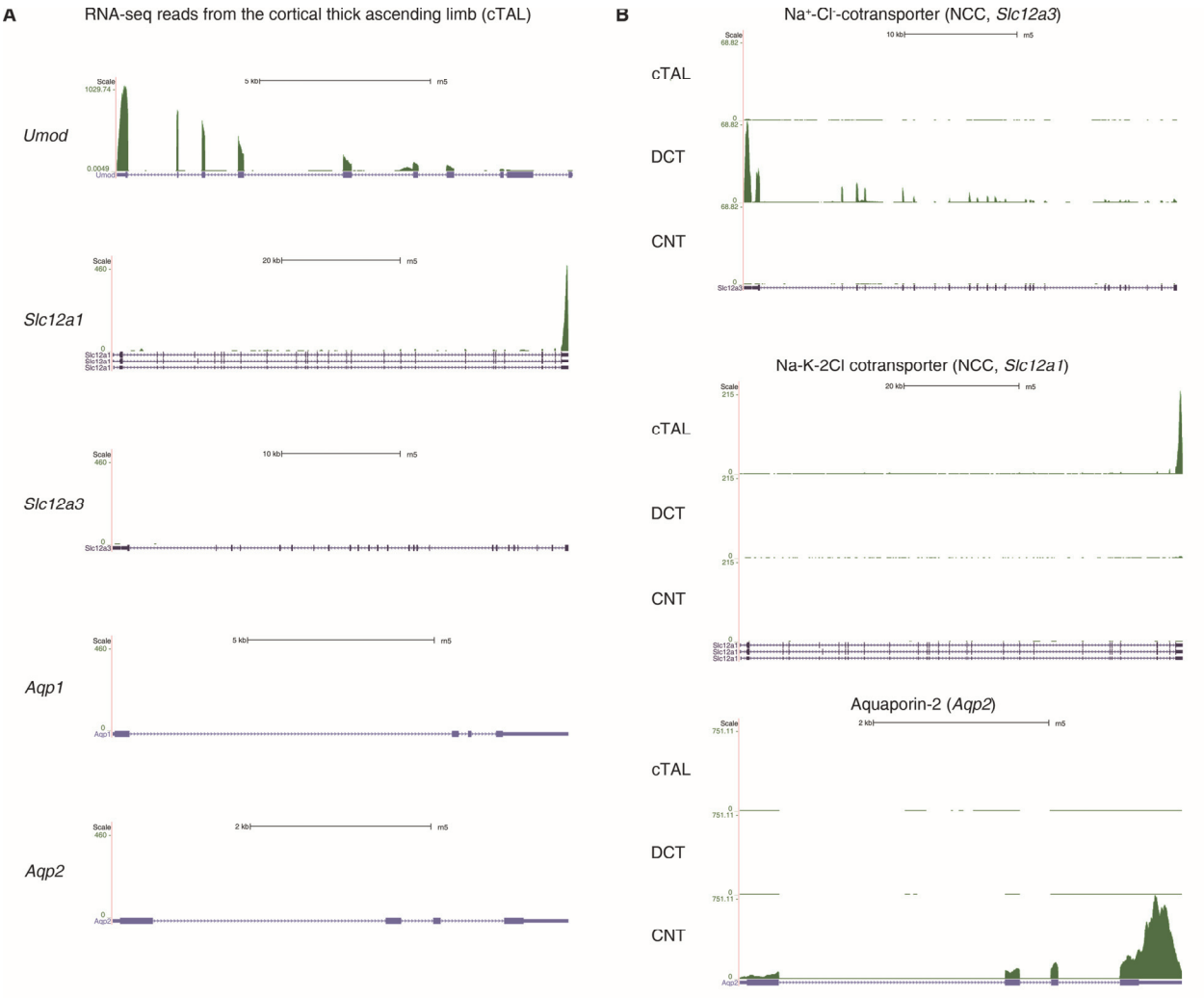

Supplemental Figure 1. RNA-seq of microdissected cortical thick ascending limbs and adjacent segments. A. RNA-seq reads from microdissected cortical thick ascending limbs (cTAL). The distribution of reads along the gene body is depicted as green histograms, aligned with diagram showing intron-exon structure. Direction of transcription is indicated by arrows. Classical markers for cTAL (*Umod* and *Slc12a1*), are highly expressed, whereas markers for neighboring segments (*Slc12a3,* distal convoluted tubule; *Aqp1,* proximal convoluted tubule; and *Aqp2,* cortical collecting duct) are not expressed. **B.** Expression of *Slc12a3*, *Slc12a1*, and *Aqp2* in the cTAL, distal

convoluted tubule (DCT), and connecting tubule (CNT). *Slc12a3* is highly expressed in the DCT, and not in the cTAL and CNT. *Aqp2* is exclusively expressed in the CNT.

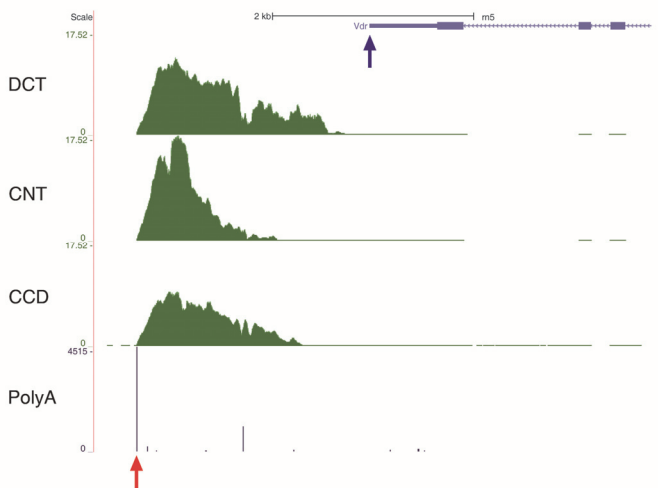

Supplemental Figure 2. Mapped RNA-seq reads for vitamin D receptor (*Vdr*). Note that most reads mapped to sites downstream from the RefSeq-annotated 3'-end (blue arrow). The distal end of this region matches the polyadenylation peak (red arrow) as called by PA-seq. These additional reads were included in the calculation of RPKMs (Datasets S3 and S4).

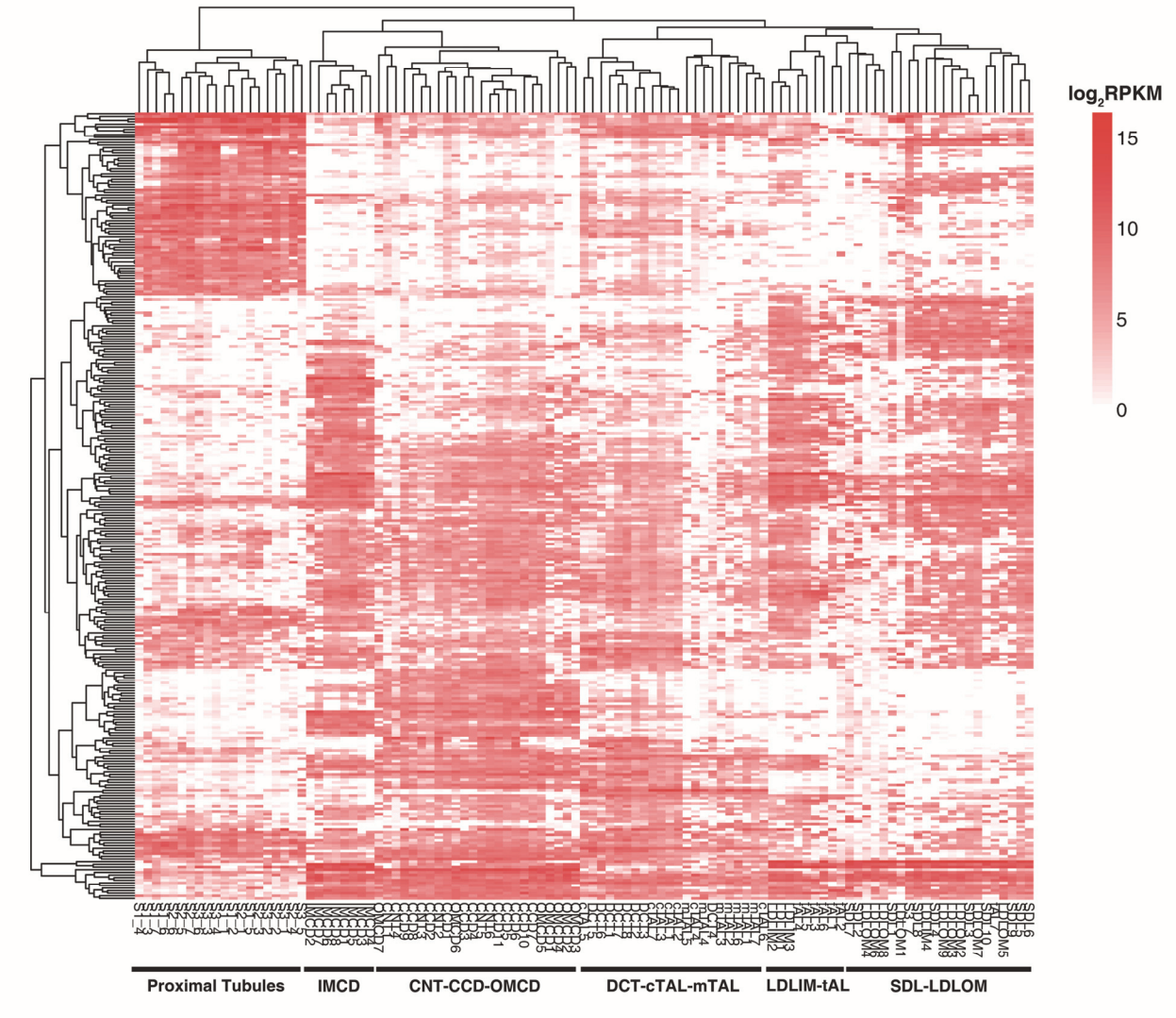

Supplemental Figure 3. A heatmap for all replicates of dissected renal tubule segments. All replicates are represented in columns, and the top 300 genes with highest variance in log_2RPKM were selected to draw this heatmap. Replicates from the same tubule segment clustered more closely with each other than with those from other segments. Replicates from 14 different renal tubule segments were found to form 6 distinct clusters according to their anatomical organization (shown by horizontal bars at the bottom of the heatmap).

A

	Gene symbol	S1	S2	S3	SDL	LDLOM	LDLIM	tAL	mTAL	cTAL	DCT	CNT	CCD	OMCD	IMCD
αENaC	*Scnn1a*	0.5	0.2	0.1	0.1	0.1	0.1	0.1	10.8	39.2	68.9	88.2	104.2	47.2	0
βENaC	*Scnn1b*	0	0.1	0	0	0	0.1	0	0.1	2.8	32	160.1	190.9	110.5	0.1
γENaC	*Scnn1g*	0	0.1	0	0	0	0	0	0	0	0.2	52.9	88.7	61.1	0

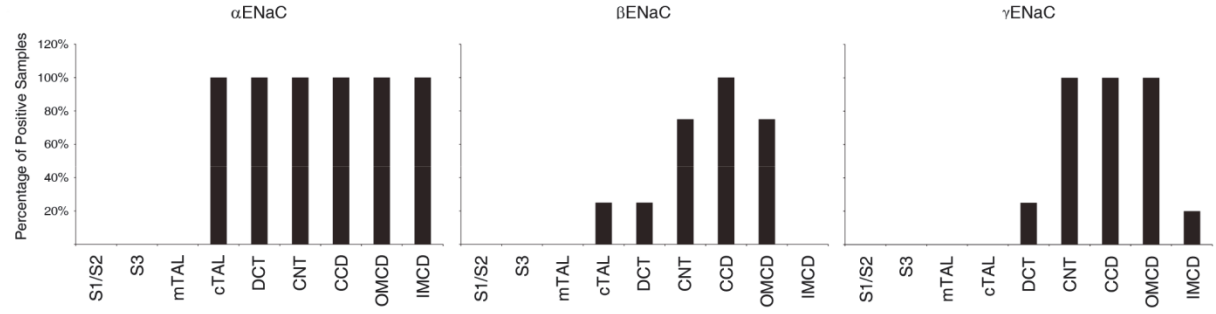

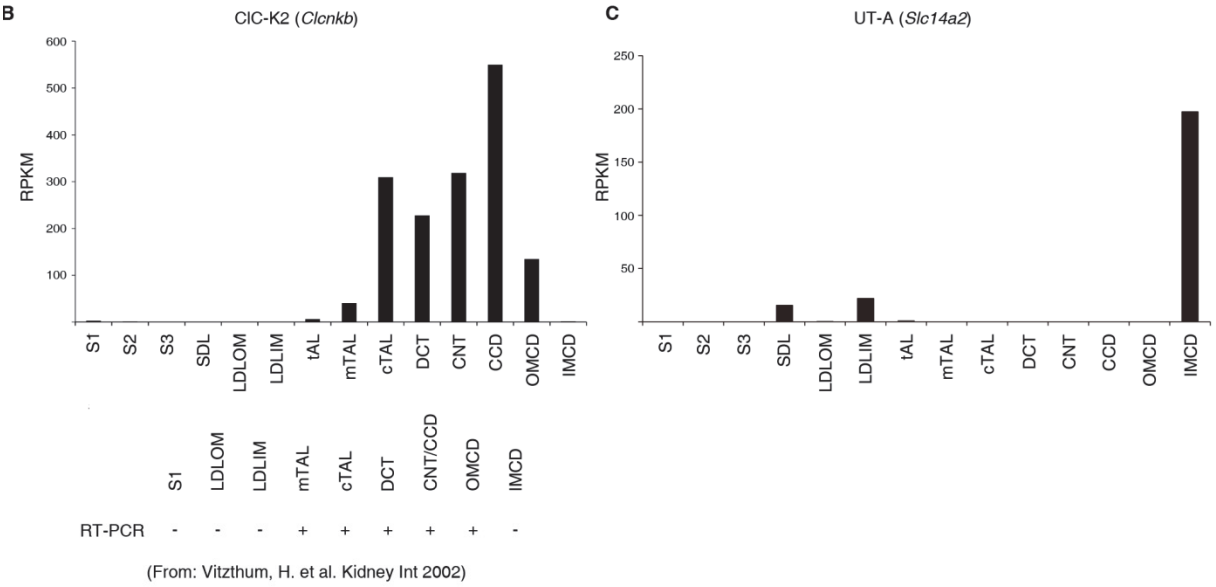

	S1	LDLOM	LDLIM	mTAL	cTAL	DCT	CNT/CCD	OMCD	IMCD
RT-PCR	-	-	-	+	+	+	+	+	-

(From: Vitzthum, H. et al. Kidney Int 2002)

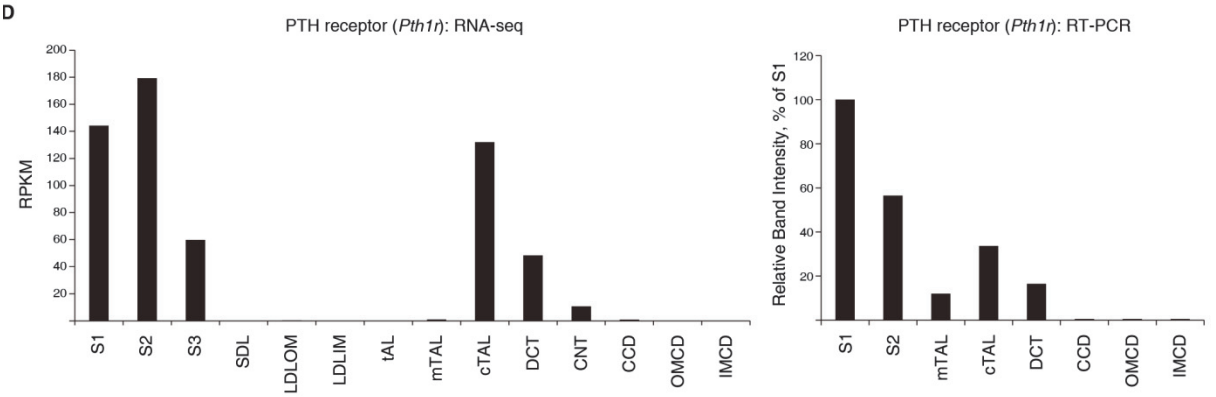

Supplemental Figure 4. Comparison of Results from Single-Tubule RNA-seq with RT-PCR Results for Specific Gene Targets. **A.** (top) Median RPKMs for subunits of the

epithelial sodium channel (ENaC). (Bottom) relative expression of ENaC subunits across renal tubule segments. **B.** RT-PCR expression level of chloride channel ClC-K2 (*Clcnkb*). **C.** RT-PCR expression level of urea transporter UT-A (*Slc14a2*). **D.** Comparison of RNA-seq and RT-PCR results for parathyroid receptor (*Pth1r*).

Supplemental Figure 5. A heatmap for expression of transcription factors along the renal tubule segments.

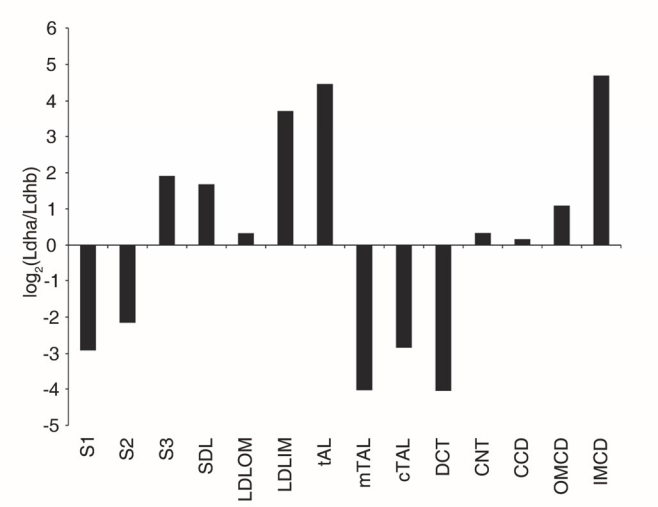

Supplemental Figure 6. Relative expression of two lactate dehydrogenase isoforms, *Ldh* and *Ldhb* along renal tubule.

Supplemental Data

Because of the large size of the datasets, we make the supplemental datasets available via a link to a publicly accessible web server. Please click on the links to access data: https://helixweb.nih.gov/ESBL/Database/NephronRNAseq/Supplemental.html (temporary login ID: clp password: Esbl!@#$)

Supplemental Data 1. Information on microdissected glomeruli and tubule segments and gene expression in each tubule segment. The tab "Microdissected tubule" contains the information on all samples of microdissected tubule segments. "RPKM_withoutPAseq" contains RPKMs for RefSeq transcripts calculated without considering PA-seq data. "RPKM_withPAseq" contains RPKMs for RefSeq transcripts supplemented with PA-seq data. The RNA-seq reads between the annotated 3'-end and the polyadenylation peak were included in the calculation of RPKMs.

Supplemental Data 2. This file contains information on chromosomal coordinates of polyadenylation-site peaks found by PA-seq. Since PA-seq is a strand-specific RNA-seq protocol, peaks on forward and reverse strands are presented on separate tabs.

Supplemental Data 3. This file contains genes that are enriched in the nephron- and collecting-duct segments. The result of DAVID analysis is stored in multiple tabs.

Supplemental Data 4. This file contains genes that are enriched in the renal medullary segments. Medulla-enriched genes and result of DAVID analysis are stored in multiple tabs.